OPEN

Citation: Cell Death and Disease (2013) 4, e715; doi:10.1038/cddis.2013.222

www.nature.com/cddis

ER stress-mediated apoptosis induced by celastrol in cancer cells and important role of glycogen synthase kinase-3β in the signal network

L Feng[1], D Zhang[1], C Fan[1], C Ma[2], W Yang[3], Y Meng[1], W Wu[1], S Guan[1], B Jiang[1], M Yang[1], X Liu*[,1] and D Guo*[,1]

HeLa cells treated with celastrol, a natural compound with inhibitive effect on proteasome, exhibited increase in apoptotic rate and characteristics of apoptosis. To clarify the signal network activated by celastrol to induce apoptosis, both the direct target proteins and undirect target proteins of celastrol were searched in the present study. Proteasome catalytic subunit β1 was predicted by computational analysis to be a possible direct target of celastrol and confirmed by checking direct effect of celastrol on the activity of recombinant human proteasome subunit β1 *in vitro*. Undirect target-related proteins of celastrol were searched using proteomic studies including two-dimensional electrophoresis (2-DE) analysis and iTRAQ-based LC-MS analysis. Possible target-related proteins of celastrol such as endoplasmic reticulum protein 29 (ERP29) and mitochondrial import receptor Tom22 (TOM22) were found by 2-DE analysis of total cellular protein expression profiles. Further study showed that celastrol induced ER stress and ER stress inhibitor could ameliorate cell death induced by celastrol. Celastrol induced translocation of Bax into the mitochondria, which might be related to the upregulation of BH-3-only proteins such as BIM and the increase in the expression level of TOM22. To further search possible target-related proteins of celastrol in ER and ER-related fractions, iTRAQ-based LC-MS method was use to analyze protein expression profiles of ER/microsomal vesicles-riched fraction of cells with or without celastrol treatment. Based on possible target-related proteins found in both 2-DE analysis and iTRAQ-based LC-MS analysis, protein–protein interaction (PPI) network was established using bioinformatic analysis. The important role of glycogen synthase kinase-3β (GSK3β) in the signal cascades of celastrol was suggested. Pretreatment of LiCL, an inhibitor of GSK3β, could significantly ameliorate apoptosis induced by celastrol. On the basis of the results of the present study, possible signal network of celastrol activated by celastrol leading to apoptosis was predicted.

Cell Death and Disease (2013) **4,** e715; doi:10.1038/cddis.2013.222; published online 11 July 2013
Subject Category: Experimental Medicine

Celastrol is a natural triterpenoid compound isolated from 'Thunder of God Vine' (*Tripterygium wilfordii* Hook. f.), a traditional Chinese medicine, which has been used successfully for centuries in treating autoimmune diseases and chronic inflammation.[1] The chemical structure of celastrol is shown in Figure 1a. Recently, the anticancer activities of celastrol attracted the interests of researchers, and celastrol was even considered as one of the most promising medicinal molecules isolated from the plant extracts of traditional medicines.[2] Interestingly, celastrol induced cell death in cancer cells, whereas it activated cytoprotection reaction in nontransformed cells.[3,4] The mechanism of celastrol was still not fully clear. The difficulty in clarifying the mechanism of celastrol resulted from the capacity of celastrol to act as a multi-target compound. The chemical structure characteristic (triterpene quinine methide) of celastrol enables it to react with the nucleophilic thiol groups of cysteine residues in proteins and form covalent Michael adducts.[5] The unclear anticancer mechanism of celastrol impeded the development of celastrol as a new anticancer drug.

Many reports have shown that celastrol, as a cytotoxic agent, induced apoptosis in cancer cells.[6–15] In our previous report, we found that celastrol could induce different kinds of cell death including apoptosis, autophagy and paraptosis in cancer cells.[6] Importantly, our study using inhibitors of apoptosis, autophagy and paraptosis indicated that apoptosis was the type of cell death that mainly contributed to the cytotoxicity of celastrol.[6] Caspase inhibitor, z-VAD-FMK, could significantly ameliorate cell death induced by celastrol.[6] In the present study, we tried to clarify the signal network by which celastrol induce apoptosis in HeLa cells. Celastrol, as a multi-target compound, might have different direct targets and

[1]Shanghai Institute of Materia Medica, Chinese Academy of Sciences, Shanghai 201203, PR China; [2]School of Life Sciences and Technology, Tongji University, Shanghai 200092, PR China and [3]Yunnan Pharmacological Laboratories of Natural Products, Kunming Medical College, Kunming 650031, PR China
*Corresponding author: X Liu or D Guo, Shanghai Institute of Materia Medica, Chinese Academy of Sciences, 501 Hai-Ke Road, Shanghai 201203, PR China. Tel: +86 21 50272789; Fax: +86 21 50272789; E-mail: xuanliu@mail.shcnc.ac.cn or daguo@mail.shcnc.ac.cn
Keywords: celastrol; apoptosis; endothelium reticulum; proteomics; bioinformatics
Abbreviations: 2-DE, two-dimensional electrophoresis; ER, endothelium reticulum; TOM, translocase of outer mitochondrial membrane; PPI, protein–protein interaction; GSK3β, glycogen synthase kinase-3β; TCM, traditional Chinese medicine; PARP, poly(ADP-ribose) polymerases; XIAP, X-linked inhibitor of apoptosis protein; MOE, molecular operating environment; TOM22, mitochondrial import receptor Tom22; ERP29, endoplasmic reticulum protein 29; PERK, pancreatic ER kinase; IRE1, inositol-requiring enzyme 1; ATF6, activating transcription factor-6; BiP, binding protein; CHOP, C/EBP-homologous protein; JNK, Jun kinase; HSP90, heat shock protein 90; Akt, protein kinase B; DMSO, dimethyl sulfoxide; AMC, 7-amido-4-methyl-coumarin; SCX, strong cation exchange
Received 08.11.12; revised 03.5.13; accepted 06.5.13; Edited by H-U Simon

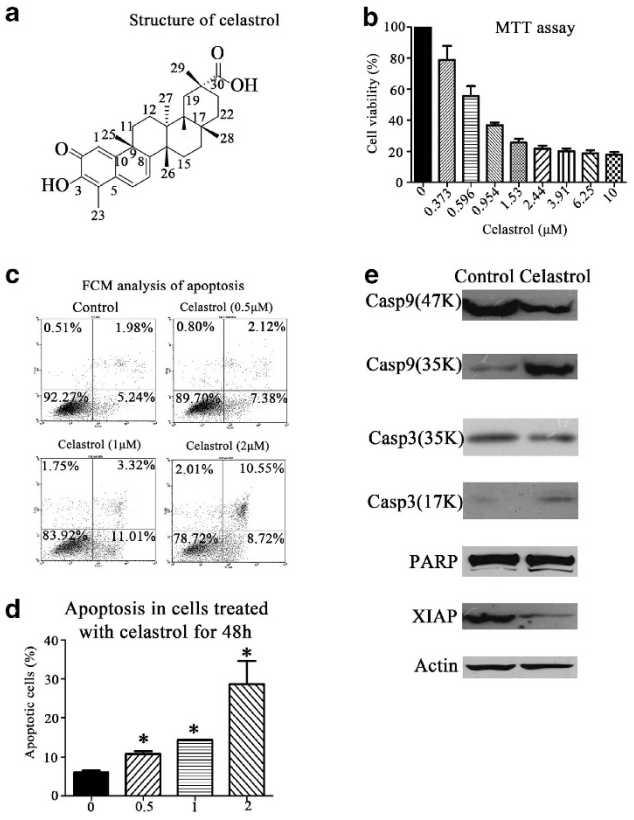

Figure 1 Celastrol inhibits cell proliferation and induces apoptosis in HeLa cells. (**a**) Structure of the celastrol molecule. (**b**) Cell viability (MTT assay) of HeLa cells treated with various concentrations of celastrol for 48 h. (**c**) Representative results of flow cytometric analysis of apoptosis in cells treated with various concentrations of celastrol for 48 h. (**d**) Statistical analysis result of flow cytometric analysis of apoptosis. Annexin V-positive cells were accepted as apoptotic cells. (**e**) Levels of caspase-9, caspase-3, poly(ADP-ribose) polymerases (PARP) and X-linked inhibitor of apoptosis protein (XIAP) in cells treated with 1 μM celastrol for 48 h. $^*P<0.05$ compared with control

could activate complicated signal cascades. However, present study would focus on its inhibiting effect on proteasome and related downstream signal cascades.

The proteasome-inhibiting capacity of celastrol was firstly reported by Yang *et al.*[16] and confirmed by researchers including ourselves.[6,17,18] However, it is unknown whether the inhibiting effect of celastrol on proteasome was direct or not. Therefore, the possibility of the three catalytic subunits of proteasome, β1, β2 and β5, to act as direct targets of celastrol was predicted using computational analysis. Then, direct effect of celastrol on the activity of recombinant proteasome β1 subunit protein *in vitro* was checked to confirm the prediction that proteasome β1 subunit might be a direct target of celastrol. Further, undirect target-related proteins of celastrol were searched in the present study using proteomic methods. Generally, it might be rational to predict the signal transduction activated by a proteasome inhibitor to be due to proteasome inhibition, then endothelium reticulum (ER) stress and finally apoptosis. However, the situation might be complicated for celastrol, as signal cascades activated by other targets of celastrol might be also involved in the effects of celastrol. Therefore, proteomic methods were used in the present study to provide relatively comprehensive and unbiased information about the target-related proteins involved in the effects of celastrol. Based on the results of proteomic analysis and in depth study of the effects of celastrol on the ER and mitochondria, signal cascades activated by celastrol leading to apoptosis were sequentially clarified.

Results

Celastrol inhibited cell proliferation and induced apoptosis in HeLa cells. As shown in Figure 1b (MTT assay result), celastrol inhibited the proliferation of HeLa cells in a dose-dependent manner. The IC_{50} value was 0.79 ± 0.22 μM (48 h treatment). Representative results of AnnexinV-FITC/propidium iodide double staining results are shown in Figure 1c, and statistical analysis results are shown in Figure 1d. The results indicated that celastrol induced apoptosis and caused an increase in the percentage of apoptotic cells. Further, western blotting assay results (Figure 1e) also showed that celastrol induced the activation of caspase-9 and caspase-3, cleavage of poly (ADP-ribose) polymerase and decrease in level of the anti-apoptotic protein X-linked inhibitor of apoptosis protein .

Effects of celastrol on the activities of cellular proteasome and finding of proteasome catalytic subunit β1 as a direct target of celastrol. As shown in Supplementary Figure 1, celastrol could inhibit all three types of cellular proteasome enzyme activities (peptidyl glutamyl-like activity, trypsin-like activity and chymotrypsin-like activity), which were mediated by catalytic subunits β1, β2 and β5, respectively. Interestingly, among the three catalytic subunits of proteasome, only the activity of β1 could be significantly inhibited by celastrol even at a low dose of 0.2 μM. The dose-dependent effects of celastrol on the activity of cellular proteasome catalytic subunit β1 were further examined (Figure 2a). As shown in Figure 2a, celastrol could dose-dependently inhibit the activity of cellular proteasome catalytic subunit β1. Further, in computational prediction of the possible binding energy between celastrol and the three catalytic subunits of bovine proteasome (β1, β2 and β5), the binding scores were -66.087341, -61.939331 and -64.804413, respectively. The results suggested that, among the three catalytic subunits, β1 subunit might have the strongest binding affinity with celastrol. The illustration of the predicted binding model and the binding sites between celastrol and proteasome β1 subunit are shown in Figures 2b and c, respectively. To confirm the direct effect of celastrol on proteasome catalytic subunit β1, recombinant human proteasome β1 subunit was expressed in *Escherichia coli* and its catalytic activity *in vitro* was checked with or without the presence of celastrol. As shown in Figure 2d, celastrol could directly inhibit the catalytic activity of β1 subunit *in vitro*. The result indicated that celastrol had direct inhibitive effect on proteasome, and cellular proteasome inhibition could be the initial step of signal cascades activated by celastrol.

Two-dimensional electrophoresis analysis result. The protein expression profiles of total cellular protein extracts of

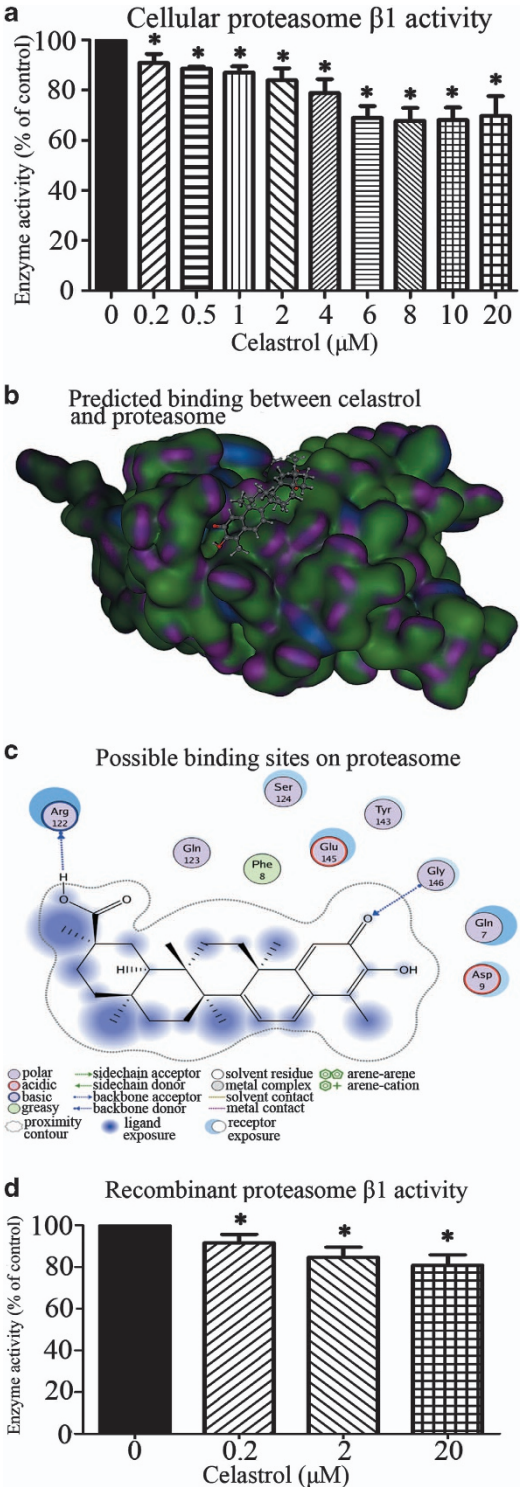

Figure 2 Inhibiting effect of celastrol on proteasomal activity and possible direct interaction with proteasome catalytic subunit β1. (**a**) Cellular proteasome catalytic subunit β1 activities of control HeLa cells and cells treated with celastrol at different concentrations for 24 h. (**b**) Illustration of predicted binding between celastrol molecule and bovine proteasome chain H (subunit β1) by MOE program. The GAD molecule is displayed in ball and stick model, whereas the protein is in surface model. (**c**) Illustration of the possible binding sites between celastrol molecule and bovine proteasome chain H (subunit β1). (**d**) Activities of recombinant human proteasome catalytic subunit β1 *in vitro* with or without the presence of celastrol. $^*P<0.05$ compared with control

cells with or without celastrol treatment were checked using two-dimensional electrophoresis (2-DE) analysis. Representative 2-DE gel images for control and celastrol-treated cells (1.0 μM for 48 h) are shown in Figure 3a. Six upregulated protein spots and four downregulated protein spots were found as indicated by the arrowed spots in Figure 3a and by the expanded plots in Figure 3b. Table 1 shows the intensity values (average and their s.d.'s) of the spots and the fold differences. The fold difference was represented by the ratio of the intensity value of celastrol-treated group to the value of control group. The differentially expressed protein spots were then identified using MS/MS. The results of MS/MS analysis are also shown in Table 1. The protein score, coverage and best ion score of each spot are shown in Table 1. The subcellular locations of the proteins are also shown in Table 1. Notably, besides three proteins located in the cytoplasm and one secreted protein, other six proteins were located in the mitochondria (three proteins), ER (1 protein), proteasome (1 protein) and nucleus (1 protein). The results suggested the involvement of these organelles in the effects of celastrol.

Induction of ER stress by celastrol and influence of ER stress inhibitor on cytotoxicity of celastrol. To confirm the results of proteomic study, the level of ER protein 29 (ERP29), a possible target-related protein of celastrol found in 2-DE analysis, was checked using western blotting assay. As shown in Figure 4a, the protein level of ERP29 was increased in celastrol-treated cells compared with control. The results were consistent with the result of 2-DE analysis. As ERP29 is a ER stress-activated protein, an increase in its expression level indicated that ER stress might be induced in celastrol-treated cells. Therefore, the influence of celastrol on ER stress markers was further observed. The time-dependent changes of ER stress-related proteins including pancreatic ER kinase (PERK), inositol-requiring enzyme 1 (IRE1), binding protein (Bip/GRP78), C/EBP-homologous protein (CHOP), caspase-4, phosphorylated Jun kinase (p-JNK), phosphorylated IRE1 (p-IRE1), phosphorylated eIF2α (p-eIF2α) and XBP1s are shown in Figure 4b. As shown in Figure 4b, celastrol treatment induced the activation of all three branches of ER stress (PERK, IRE1 and Bip). Signal proteins downstream of ER stress, such as eIF2α, CHOP, JNK, XBP1s and caspases-4, were also activated. Further, pretreatment of ER stress inhibitor salubrinal could partly inhibit the cytotoxicty of celastrol (Figure 4c). The results suggested the involvement of ER stress in cytotoxicity of celastrol.

Celastrol induced translocation of Bax into mitochondria and the role of BH-3-only proteins in linking ER stress and mitochondrial apoptosis. As shown in Figure 5a, consistent with the results of proteomic analysis, protein level of mitochondrial import receptor Tom22 (TOM22) was upregulated by celastrol. The increase of TOM22 induced by celastrol could be observed in the protein extract of whole cells and was obvious in that of mitochondria fraction. At the same time, the level of the pro-apoptotic protein Bax in the mitochondria fraction was also increased by celastrol (Figure 4a). Results of real-time PCR

analysis (Figure 5b) showed that celastrol upregulated mRNA levels of almost all the translocase of outer mitochondrial membrane (TOM) complex members except TOM70. Among the TOM proteins, TOM22 exhibited the strongest increase. The translocation of Bax into the mitochondria induced by celastrol is clearly shown in Figure 5c. In the control cells, GFP-Bax signal (green fluorescence) was distributed diffusely in the cytoplasm. On the contrary, in celastrol-treated cells, Bax became punctate and was colocalized with mitochondria (red fluorescence). The statistical analysis of the percentage values of colocalization is also shown in Figure 5c. The results indicated that celastrol activated mitochondria-based Bax translocation, which might induce apoptosis. To check whether BH-3-only proteins were involved in the signal transduction between ER stress and mitochondrial apoptosis, the expression levels of BH-3-only proteins were checked using real-time PCR. As shown in Figure 5d, among the eight BH-3-only proteins, the expression levels of BIM and PUMA were increased in celastrol-treated cells. Further work using siRNA for BIM showed that RNAi of BIM could ameliorate the increase of TOM22 (Figure 5e) induced by celastrol treatment. Moreover, RNAi of BIM could also partly inhibit apoptosis induced by celastrol treatment (Figure 5f).

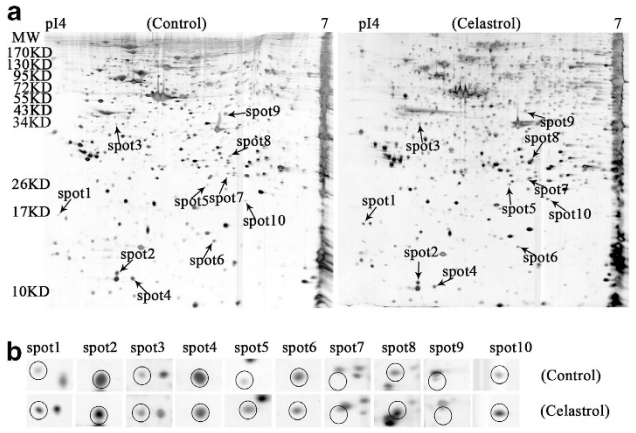

Figure 3 Results of 2-DE analysis of cellular protein expression profiles of control cells and cells treated with celastrol. (**a**) Representative 2-DE gel images of control, celasrol (1 μM)-treated groups. Differentially expressed spots are shown by the arrows. (**b**) The expanded region of differentially expressed protein spots in (**a**). The proteins within the circles were the differentially expressed proteins

Differentially expressed proteins in ER/microsomal vesicles-riched fraction of celastrol-treated cells compared with control. Because of the important role of ER stress in the effects of celastrol, proteomic analysis (iTRAQ-based LC-MS) was conducted to check the influence of celastrol on protein expression profiles of ER/microsomal vesicles-rich fraction of cells. In the present study, totally 1999 unique proteins with $\geq$2 unique peptides were

Table 1 Summary of differentially expressed proteins under celastrol treatment and the results of protein identification using MALDI-TOF MS/MS

Spot	Target protein name	NCBI accession number	*Mr* (Da)	pI	Protein score	Sequence coverage (%)	Best ion score	Spot volume (ppm)		Fold difference	Subcellular location
								Control	Celastrol treated		
1	Mitochondrial import receptor Tom22	gil9910382	15511.8	4.27	115	66	43	304.0 ± 254.6	527.5 ± 169.5	1.74	Mitochondria outer membrane
2	Cytochrome c oxidase subunit Va	gil18999392	16751.7	6.3	169	36	48	2638.1 ± 942.8	1533.0 ± 758.9	0.58	Mitochondria inner membrane
3	Eukaryotic translation elongation factor 1 delta isoform 2	gil25453472	31102.8	4.9	180	54	50	183.4 ± 73.8	299.2 ± 122.4	1.63	Cytoplasmic and nuclear
4	Galectin-1	gil42542977	14583.2	5.34	88	38	37	2196.9 ± 988.1	1146.8 ± 501.7	0.52	Secreted, extracellular space
5	Proteasome subunit beta type-4	gil48145757	29171.5	5.7	216	51	53	252.6 ± 99.7	411.0 ± 152.9	1.63	Proteasome
6	Stathmin 1	gil62088144	15093	8.47	70	26	36	942.1 ± 356.6	437.5 ± 204.3	0.46	Cytoplasm, cytoskeleton
7	NAD(P)H dehydrogenase, quinone 2	gil56205043	21523.8	6.07	217	56	56	375.8 ± 166.9	628.2 ± 245.7	1.67	Cytoplasm
8	Endoplasmic reticulum protein 29 isoform 1 precursor	gil5803013	28975.2	6.77	158	33	29	416.7 ± 226.8	786.6 ± 387.1	1.89	Endoplasmic reticulum lumen
9	Isocitrate dehydrogenase 3 (NAD+) alpha precursor	gil5031777	39566.1	6.47	234	37	50	1392.7 ± 773.3	674.3 ± 287.2	0.46	Mitochondrial matrix
10	Splicing factor, arginine/serine-rich 3	gil4506901	19317.9	11.6	216	52	36	186.5 ± 83.3	367.8 ± 215.9	1.97	Nucleus

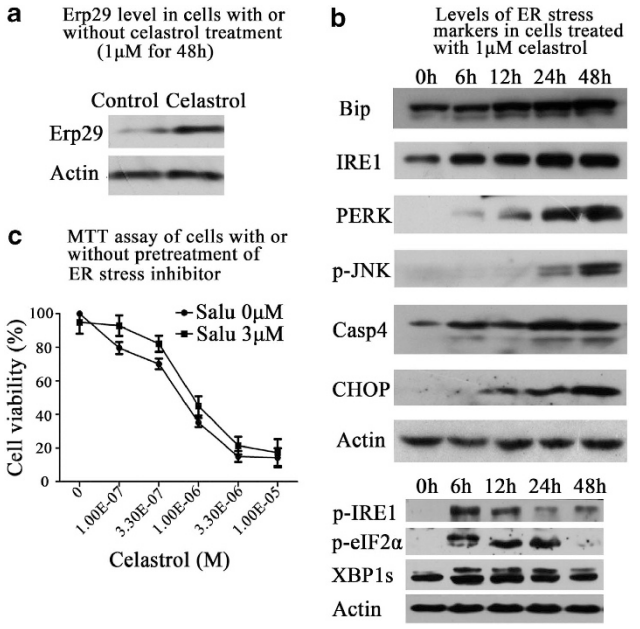

Figure 4 Effects of celastrol on ER stress-related proteins and influence of ER stress inhibitor on cytotoxicity of celastrol. (**a**) Results of western blotting assay of protein levels of ERP29 in control cells and cells treated with 1 μM celastrol for 48 h. (**b**) Results of western blotting assay of levels of ER stress-related proteins in control cells and celastrol-treated cells (1 μM for different time periods). (**c**) Results of trypan blue exclusion assay of cell viability of celastrol-treated (48 h at different concentrations) cells with or without pretreatment of 3 μM salubrinal for 0.5 h. *$P<0.05$ compared with control

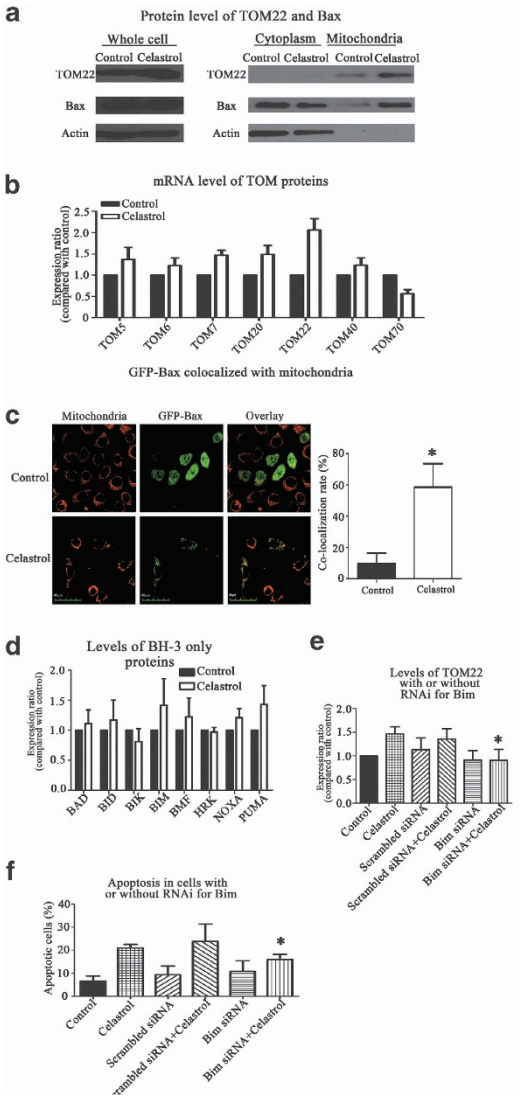

Figure 5 Effects of celastrol on mitochondrial TOM complex, Bax translocation and BH-3-only proteins. (**a**) Results of western blotting assay of protein levels of TOM22 and Bax in control cells and cells treated with 1 μM celastrol for 48 h. The levels of TOM 22 and Bax in protein samples of whole cell, cytoplasm fraction and mitochondria fraction were examined. (**b**) Results of PCR analysis of mRNA levels of members of TOM complex in control cells and celastrol-treated cells (1 μM celastrol for 24 h). (**c**) Results of confocal laser scanning microscope observation of Bax translocation from cytoplasm to mitochondria in celastrol-treated cells (1 μM celastrol for 24 h). Both the representative and the statistical analysis results are shown. *$P<0.05$ compared with control. (**d**) Results of PCR analysis of mRNA levels of BH-3-only proteins in control cells and celastrol-treated cells (1 μM celastrol for 24 h). (**e**) Results of PCR analysis of mRNA levels of TOM22 in control cells and cells treated with scrambled siRNA or siRNA for BIM. For celastrol treatment, cells were treated with 1 μM celastrol for 24 h. *$P<0.05$ compared with celastrol-treated control cells. (**f**) Results of flow cytometry analysis of apoptosis in control cells and cells treated with scrambled siRNA or siRNA for BIM. For celastrol treatment, cells were treated with 2 μM celastrol for 24 h. Annexin V-positive cells were accepted as apoptotic cells. *$P<0.05$ compared with celastrol-treated control cells

identified (Supplementary Table S1). Totally, 162 proteins with at least 1.5-fold change between the control and celastrol-treated group were found (Supplementary Table S2). GO analysis of the 162 differentially expressed proteins is shown in Supplementary Table S3. Only GO terms containing more than five proteins are listed. As shown in Supplementary Table S3, celastrol treatment induced changes in pathways, mainly including cellular response to stress, proteasomal ubiquitin-dependent process, cell proliferation and cell death, regulation of gene expression, cytoskeleton organization and cell motility.

Possible protein–protein interaction network of celastrol. Protein–protein interaction (PPI) network was established based on the total 172 possible target-related proteins of celastrol including the 10 proteins found in 2-DE analysis and 162 proteins found in iTRAQ-based LC-MS analysis. Among the 172 proteins, 152 of them can link together into one network through direct interaction or only through one intermediate partner at the PPI level, as shown in Figure 6a. The full names of the intermediate partners in the network are shown in Supplementary Table S4. Interestingly, In this network, glycogen synthase kinase-3β (GSK3β) exhibited to be the target-related protein that had the most numerous connections with other proteins in the signal network (Figure 6b). The results suggested that GSK3β might be a critical factor in the effects of celastrol.

Confirmation of the involvement of GSK3β in the effects of celastrol. Western blotting assay result (Figure 6c) showed the time-dependent change of GSK3β under celastrol treatment. The result indicated that the protein level of GSK3β was decreased by celastrol treatment. The result was consistent with the result of iTRAQ-based LC-MS

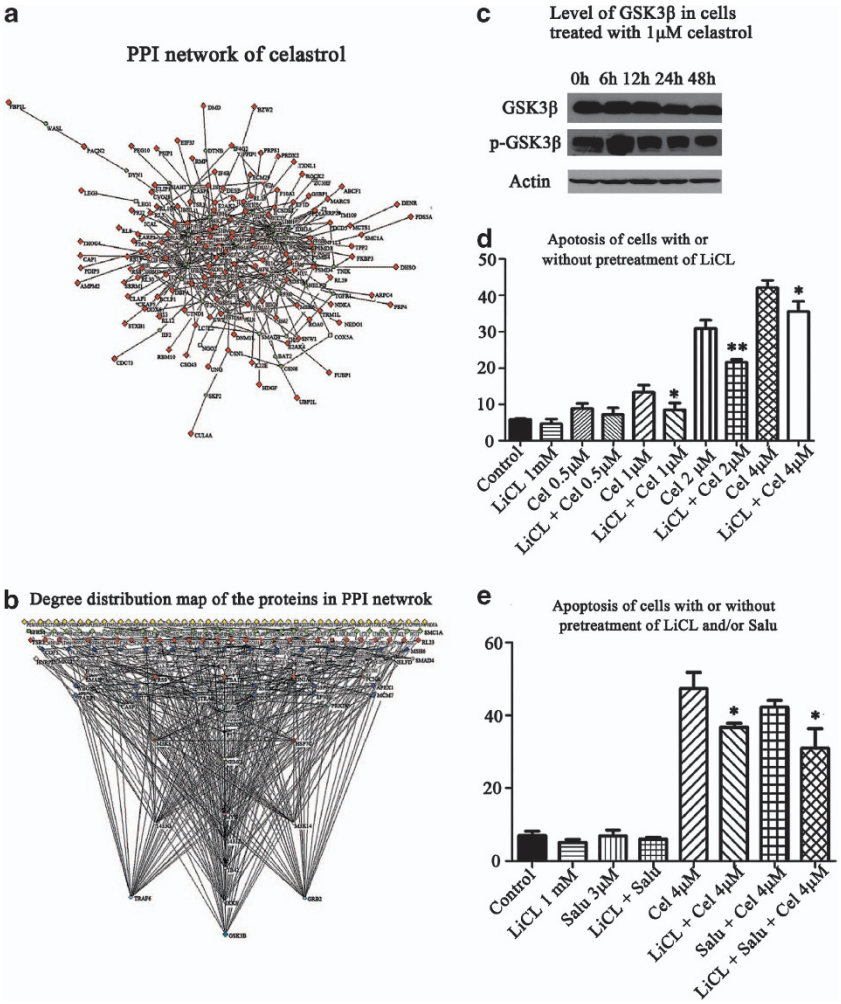

Figure 6 Role of GSK3β in signal network of celastrol and celastrol-induced apoptosis. (**a**) The constructed minimum PPI network of celastrol containing 152 experimental identified proteins found in 2-DE and LC-MS and 34 intermediate proteins. The 152 proteins (red diamonds for LC-MS and cyan box dots for 2-DE) can link together into one network through direct interaction or only one intermediate partner (green ellipse dots). (**b**) Degree distribution map of the proteins in PPI network of celastrol. Experimental identified proteins are shown as diamonds, whereas the intermediate proteins are shown as round dots. In this graph, the colors were only related to degree in the network. GSK3β exhibited to have the biggest degree in all experimental identified proteins. (**c**) Results of western blotting assay of time-dependent change in protein levels of GSK3β and p-GSK3β (ser9) in cells treated with 1 μM celastrol. (**d**) Statistical analysis result of flow cytometric analysis of apoptosis in celastrol-treated cells (0.5, 1, 2, 4 μM celastrol for 48 h) with or without pretreatment of LiCL (1 mM for 1 h). Annexin V-positive cells were accepted as apoptotic cells. *$P<0.05$ compared with corresponding celastrol-treated group without pretreatment. (**e**) Statistical analysis result of flow cytometric analysis of apoptosis in celastrol-treated cells (4 μM celastrol for 48 h) with or without pretreatment of LiCL (1 mM for 1 h) and/or salubrinal (3 μM for 0.5 h). Annexin V-positive cells were accepted as apoptotic cells. *$P<0.05$ compared with the corresponding celastrol-treated group without pretreatment

analysis. Further, the activation state of GSK3β was also checked. As shown in Figure 6c, after celastrol treatment, Ser (9) phosphorylation of GSK3β was increased at 6 and 12 h, but decreased subsequently at 24 and 48 h. To check whether the change in GSK3β was only a consequence of apoptosis or not, the effect of topotecan, a classical apoptosis inducer, on GSK3β was also checked and compared with that of celastrol. As shown in Supplementary Figure S2, after 48-h treatment, the level of p-GSK3β was decreased in celastrol-treated cells but increased in topotecan-treated cells. The results indicated that the activation of GSK3β by celastrol was not a consequence of apoptosis. To confirm the role of GSK3β in the effects of celastrol, LiCL, a GSK3β inhibitor, was used in the present study. The capacity of LiCL to inhibit GSK3β is shown in Supplementary Figure S3. LiCL at 1, 2 or 5 mM all could inhibit GSK3β. The influence of pretreatment of LiCL (1 mM for 1 h) on celastrol-induced apoptosis is shown in Figure 6d. Pretreatment of LiCL could significantly decreased the percentage values of apoptotic cells after celastrol treatment. Further, co-treatment of salubrinal, a ER stress inhibitor, with LiCL could further decrease the percentage values of apoptotic cells after celastrol treatment though the difference was not significant compared with LiCL treatment alone (Figure 6e).

Signal network by which celastrol induced apoptosis. On the basis of the above results, a schematic illustration of the signal network by which celastrol induced apoptosis could be summarized (as shown in Figure 7).

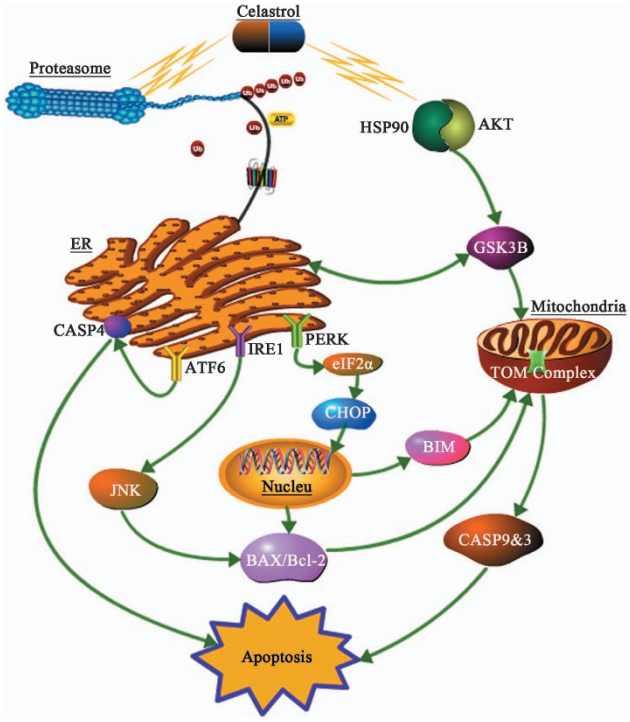

Figure 7 A schematic illustration of signal network in which celastrol induced apoptosis

Discussion

Consistent with previous reports, apoptosis was induced in HeLa cells treated with celastrol. Inhibiting effects of celastrol on proteasomal activities were also observed. By using computational prediction and recombinant human proteasome catalytic subunit β1, we found in the present study that proteasome catalytic subunit β1 could serve as a direct target of celastrol. The results suggested that the inhibiting effect of celastrol on proteasome was direct, and signal cascades downstream of proteasome inhibition might be activated by celastrol. Results of proteomic analysis of cellular protein expression profiles in cells with or without celastrol treatment suggested possible target-related proteins of celastrol such as ERP29, a ER stress-activated protein, and TOM22, a mitochondrial membrane protein. The regulation of ERP29 and TOM22 by celastrol was confirmed. ERP29 is an ER-resident chaperone that facilitates processing and transport of proteins.[19] Increased expression of ERP29 could result in transcriptional activation of genes with tumor suppressive function and lead to cell growth arrest.[20] The increase of ERP29 in celastrol-treated cells suggested the induction of ER stress by celastrol. To be noted, the possible inducing effect of celastrol on ER stress was first reported in our previous report.[6] However, only in the present study, the effect of celastrol on ER stress was studied in depth. Celastrol induced activation of the three branches of ER stress and related signal proteins. Increase in expression of Bip in celastrol-treated cells was observed. Moreover, eIF2α and CHOP, markers of the PERK branch of ER stress,[21] were activated by celastrol. The activation of IRE1α and its downstream protein JNK[22] were also induced by celastrol. Especially, the activation of CHOP and XBP1s suggested that celastrol might induce transcription of ER stress target genes. The fact that pretreatment of salubrinal, an ER stress inhibitor, could ameliorate cell death induced by celastrol confirmed the role of ER stress in the effects of celastrol.

The finding of TOM22 as a possible target-related protein of celastrol led us to further study the translocation of Bax into mitochondria in cells treated with celastrol. TOM complex on the outer membrane of mitochondria was the entry gate for the proteins that were imported into the mitochondria[23] and was also found to be necessary for tBid/Bax-induced cytochrome C release.[24,25] Especially, among the members of TOM complex, TOM22 had been accepted as a mitochondrial receptor for Bax[26] and the cytosolic domain of TOM22 could modulate the mitochondrial translocation and conformation of Bax.[27] Celastrol induced an increase in both mRNA level and protein level of TOM 22. Moreover, consistent with the increase in TOM22 level, translocation of Bax into mitochondria was observed in celastrol-treated cells. These results suggested the involvement of TOM22 and mitochondrial-dependent Bax translocation in the apoptosis induced by celastrol. However, Bax translocation independent of TOM complex had also been reported before.[28] The possibility of involvement of other factors in Bax translocation induced by celastrol could not be excluded.

To find the link between ER stress and mitochondrial apoptosis induced by celastrol, the expression levels of BH-3-only proteins were checked. The results indicated that the expression levels of BIM and PUMA were increased by celastrol. Further, siRNA for BIM could inhibit the increase in TOM22 expression induced by celastrol. BIM, is a direct link between ER stress and mitochondrial apoptosis and is essential for ER stress-induced apoptosis in a diverse range of cell types both in culture and within the whole animal.[29,30] Our results also showed that siRNA for BIM could inhibit celastrol-induced apoptosis. The expression of BIM as well as other BH-3-only proteins was reported to be regulated by CHOP.[31] Therefore, the sequential links between proteasome inhibition, ER stress, CHOP, BIM, TOM22 and Bax translocation might indicate a clear pathway of mitochondrial apoptosis induced by celastrol.

In further proteomic analysis of ER/microsomal vesicles-enriched fraction, GSK3β was found to be the possible critical target-related protein of celastrol. GSK3β is a multifunctional serine/threonine kinase, which was initially identified as a key regulator of insulin-dependent glycogen synthesis. It is now well known that GSK3β functions in diverse cellular processes including proliferation, differentiation, motility and survival and is involved in energy metabolism, neuronal cell development, body pattern formation and ER stress.[32–35] Moreover, aberrant regulation of GSK3β has been implicated in a range of human pathologies including neoplastic transformation and tumor development.[36,37] Especially, GSK3β has been recognized as an important modulator of apoptosis.[38,39] In the present study, the protein level of GSK3β was slightly decreased in celastrol-treated cells. More importantly, our results showed that there was an increase in phosphorylated GSK3β (Ser9) level at an early stage (6 h, 12 h) of celastrol treatment followed by a decrease at late stage (24, 48 h). GSK3β could be inhibited by phosphorylation (Ser9) and

activated by dephosphorylation.[40] The inhibition of GSK3β at an early stage and activation at later stage of celastrol treatment indicated that the regulation of GSK3β by celastrol was complicated. Pretreatment of LiCL, a GSK3β inhibitor,[41] could significantly ameliorate celastrol-induced apoptosis. It was reported that activation of GSK3β could be regulated by multiple factors. Proteasome inhibition[42] and ER stress[43,44] could regulate the phosphoryaltion of GSK3β. At the same time, GSK3β phosphorylation could also be regulated by heat shock protein 90 (HSP90) and protein kinase B (Akt) pathway.[45] To be noted, HSP90 was reported to be a direct target of celastrol. The direct inhibitive effect of celastrol on HSP90 and the decrease of Akt in celastrol-treated cells had been reported.[46] In our previous report, we also observed the decrease of Akt in celastrol-treated HeLa cells.[6] Therefore, we predicted that, under the concomitant regulation of HSP90/Akt and ER stress resulted from proteasome inhibition, GSK3β might be inhibited (phosphorylated) at an early stage of celastrol treatment and then activated (dephosphorylated) at late stage. By exhibiting the influence on mitochondria permeability,[47,48] Bax/Bcl-2[39,49] and caspases activation,[50] GSK3β might have critical role in the regulation of apoptosis induced by celastrol. As a joint protein regulated by different direct targets of celastrol, the important role of GSK3β in the effects of celastrol deserved further study.

Based on the results of the present study, the possible signal network by which celastrol induced apoptosis was predicted (as shown in Figure 7). One of the main findings in the present study is the clarification of the signal cascades activated by celastrol through proteasome inhibition. Briefly, by directly inhibiting proteosome activities, celastrol induced ER stress, activated CHOP and XBP1s, increased transcription of ER stress target genes such as BIM, induced Bax translocation into mitochondria and finally activated mitochondrial apoptosis. Further, a second important observation in the present study is the critical role of GSK3β in the effects of celastrol. As a multi-target compound, celastrol might activate complicated signal cascades in cells. Finding GSK3β as the critical factor in the effects of celastrol would contribute to understanding the mechanism of celastrol.

Materials and Methods

Chemicals. Celastrol with purity more than 98% was bought from Shanghai Hotmed Sciences Co. Ltd. (Shanghai, China). Celastrol was dissolved in dimethyl sulfoxide to the concentration of 0.01 M as a stock solution and kept at $-20\,^{\circ}C$. It was then diluted in the culture medium to the final concentration as indicated in every experiment. All reagents used in 2-DE analysis were purchased from Bio-Rad Laboratories (Hercules, CA, USA) and all reagents used in iTRAQ-based LC-MS were purchased from AB SCIEX Pte. Ltd. (Framingham, MA, USA). Other chemical reagents, except where specially noted, were purchased from Sigma-Aldrich (St. Louis, MO, USA).

Cell culture and cell viability assay. The human cervical carcinoma cell line HeLa (CCL-2) was obtained from the American Type Culture Collection (Rockville, MD, USA). HeLa cells were cultured in minimum essential medium supplemented with 10% fetal bovine serum, 100 U/ml penicillin and 100 mg/l streptomycin (Invitrogen, Karlsruhe, Germany). Cell viability of cells with or without celastrol treatment was measured by MTT assay or Trypan blue exclusion assay as described before.[6,51] Detailed description of MTT and Trypan blue exclusion assay can be found in Supplementary Materials and Methods.

Flow cytometric analysis of apoptosis induced by celastrol. Flow cytometric analysis of cell apoptosis was conducted using apoptosis detection kit (Calbiochem, Merck KGaA, Darmstadt, Germany) according to the manufacturer's instructions. Briefly, after treatment, cells were collected, washed with PBS and then resuspended in binding buffer and then incubated with Annexin V-FITC and propidium iodide for 15 min in the dark. Then, flow cytometric analysis was conducted using FACSCalibur Flow Cytometer and data analysis were performed with CellQuest software (BD Biosciences, Sparks Glencoe, MD, USA).

Preparation of samples of total cellular proteins and samples of mitochondria and cytoplasm fractions. Detailed information can be found in Supplementary Materials and Methods.

Western blotting assay. For western blotting assay, the protein samples were denatured by mixing with equal volume of $2\times$ sample loading buffer and then boiling at $100\,^{\circ}C$ for 5 min. An aliquot (100 μg as protein) of the supernatant was loaded onto a 12% SDS gel, separated electrophoretically and transferred to a PVDF membrane (Bio-Rad). After the PVDF membrane was incubated with 10 mM TBS with 1.0% Tween-20 and 10% dehydrated skim milk to block nonspecific protein binding, the membrane was incubated with primary antibodies overnight at $4\,^{\circ}C$. Detailed information of primary antibodies used can be found in Supplementary materials and methods. Blots were then incubated with HRP-conjugated goat anti-mouse IgG (Cell Signaling Technology, Danvers, MA, USA) or HRP-conjugated goat anti-rabbit IgG (Cell Signaling Technology) for 2 h at room temperature at a 1 : 1000 dilution and then visualized using chemiluminescence (Pierce Biotechnology, Rockford, IL, USA).

Effects of celastrol on activities of cellular proteasome and finding of proteasome catalytic subunit β1 as a direct target of celastrol. To examine the effect of celastrol on cellular proteasome activities, cells were treated with celastrol at different concentrations for 24 h, harvested, washed with PBS and then lysed with proteasome activity assay buffer (10 mM Tris-HCL, pH 7.8, 5 mM adenosine triphosphate, 0.5 mM dithiothreitol and 5 mM $MgCL_2\bullet 6H_2O$) for 30 min at $4\,^{\circ}C$. The homogenate was then centrifuged at $15\,000\times g$ for 30 min at $4\,^{\circ}C$. The supernatant was collected as whole-cell extract and the protein content in the supernatant was measured with the Bradford reagent. The enzymatic activity of cellular proteasome in cell lysate was measured similar to previous reports.[52,53] Detailed information can be found in Supplementary Materials and Methods.

The possible binding affinity between celastrol and the three proteasome catalytic subunits was predicted using molecular operating environment (MOE) program from the Chemical Computing Group Inc. as described previously.[54] As there was no information about human proteasome 3-D structure in PDB database, the 3D structure of bovine proteasome (PDB ID: 1IRU) was used. The chain H, I, L of bovine proteasome were the corresponding subunits to the human subunit β1, β2 and β5. The 3-D structure of celastrol (PubChem CID: 122724) was used for the docking simulation. The active sites on the protein chain were searched using Site Finder and dummy atoms were created from the resulting alpha spheres. The MOE-Dock default parameters were used for the docking simulation. Refinement and Rescoring 2 were set up to the Forcefield and Alpha HB, respectively.

To confirm the direct effect of celastrol on proteasome catalytic subunit β1, the recombinant human proteasome β1 (also known as PSMB6, NM_002798) was expressed. Detailed information about the expression of recombinant human proteasome β1 can be found in Supplementary materials and methods. The purified recombinant human proteasome β1 subunit was then used for enzyme activity. Briefly, catalytic activity of the recombinant human proteasome β1 subunit was assayed by adding recombinant β1 protein (50 μg) to 100 μl of assay buffer containing 50 μM Z-LLE-7-amido-4-methyl-coumarin (AMC) in the presence of celastrol at different concentrations or not. The released AMC was detected using a Microplate Reader.

2-DE analysis and MALDI-TOF MS/MS. For protein preparation, cells were cultured in 75 cm^2 flasks at a density of 2×10^5 cells/flask and treated with 1 μM celastrol. After 48 h celastrol treatment, samples of total cellular proteins were prepared as described above. 2-DE analysis and MALDI-TOF MS/MS were conducted as described in our previous reports.[51,55] Detailed information can be found in Supplementary Materials and Methods.

Detection of change in ER stress-related proteins and influence of ER stress inhibitor on cytotoxicity of celastrol. The influence of celastrol (1 μM for 48 h) on protein level of ERP29 was checked using western

blotting assay as described above. Moreover, the time-dependent change in protein levels of Bip, PERK, IRE1, CHOP, p-JNK, caspase-4, p-IRE1, p-eIF2α and XBP1s in cells with or without celastrol treatment (1 μM for 48 h) were also checked using western blotting assay. Further, to confirm the involvement of ER stress in the cytotoxicity of celastrol, cell viability of celastrol-treated cells with or without pretreatment of ER stress inhibitor salubrinal (3 μM for 0.5 h) was examined using trypan blue exclusion assay as described above.

Effects of celastrol on mitochondrial TOM complex and Bax translocation into mitochondria. The influence of celastrol (1 μM for 48 h) on protein levels of TOM22 and Bax was confirmed using western blotting assay as described above. The protein levels of TOM22 and Bax in total cellular protein, cytoplasm fraction and mitochondria fraction were all checked. The influence of celastrol (1 μM for 24 h) on mRNA expression levels of components of TOM complex including TOM5, TOM6, TOM7, TOM20, TOM22, TOM70 was examined using real-time PCR analysis. Detailed information about PCR analysis can be found in Supplementary Materials and Methods.

The influence of celastrol on Bax translocation was examined using cells transfected with GFP-Bax plasmid. The GFP-Bax plasmid was kindly provided by Professor Qi Hou (Institute of Materia Medica, Chinese Academy of Medical Sciences and Peking Union Medical College). As shown in the previous reports of Professor Qi Hou and *et al.*,[56,57] the GFP-Bax plasmid was suitable for studying Bax translocation from cytoplasm to mitochondria in apoptosis. Detailed information about transfection of GFP-Bax can be found in Supplementary materials and methods. Cells transfected with GFP-Bax were then treated with 1 μM celastrol for 24 h and stained with mitochondria-staining marker Mito-tracker M7513 (Life Technologies) according to the instructions of the manufacturer. Briefly, after PBS washes, cells were fixed in 4% paraformaldehyde for 5 min at 37 °C followed with PBS washes and then incubated with pre-warmed Mito-Tracker M7513 solution (500 nM) for 30 min at 37 °C. The fluorescence of GFP-Bax (green) and Mito-tracker M7513 (red) were observed with an Olympus confocal laser scanning microscope. Quantification of colocalization of the two labels (green and red) was conducted using the 'Colocalization' module of Imaris 7.2.3 (Bitplane AG, Saint Paul, MN, USA, www.bitplane.com). For each group, control or celastrol-treated cells, three slides from different experiments were used for quantification. For each slide, at least five fields of view were observed. A broad region of interest was defined as all the voxels in which the intensity of one of the labels was above a pixel intensity of 10 (in the 0–255 scale). Then, automatic thresholding was used to calculate the thresholds for each label. Once the thresholds were set, the program outputted the results of colocalization analysis.

Effects of celastrol on BH-3-only proteins and the role of BIM in regulation of TOM22 and apoptosis. The influence of celastrol (1 μM celastrol for 24 h) on mRNA expression levels of BH-3-only proteins were examined using real-time PCR analysis as described above. The primer pairs for tBAD, BID, BIK, BMF, HRK, NOXA and PUMA are shown in Supplementary Table S5. To check the role of BIM in regulation of TOM22 by celastrol, RNAi for BIM was conducted. The siRNAs for BIM, 5′-UCUUACGACUGUUACGUUAUUdTdT-3′ (sense) and 5′-pUAACGUAACAGUCGUAAGAUUdTdT-3′ (antisense), and negative control scrambled siRNA were synthesized by Life Tech Company (Shanghai, China). Briefly, 8×10^4/well HeLa cells were seeded into six-well plates in complete MEM medium without antibiotics. After culture overnight, cells were transfected in MEM with 40 pM scrambled siRNA or with 40 pM BIM siRNA for 24 h using the Lipofectamine RNAiMAX according to the manufacturer's instructions. After transfection, the expression of BIM in cells was checked to ensure the efficiency of BIM siRNA. Then, cells were treated with 1 μM celastrol or solvent control for 24 h and then mRNA expression levels of TOM22 were examined. The apoptosis in cells treated with scrambled siRNA, BIM siRNA, scrambled siRNA + celastrol, BIM siRNA + celastrol for 24 h was also checked using flow cytometry analysis as described above.

iTRAQ-based LC-MS analysis of protein expression profile of ER/microsomal vesicles-enriched fraction of cells with or without celastrol treatment. The ER/microsomal vesicles-enriched fraction of cells with or without celastrol treatment (1 μM celastrol for 48 h) were prepared similar to previous report.[58] Detailed information can be found in Supplementary Materials and Methods.

Bioinformatic analysis. The GO analysis was performed using DAVID database (http://david.abcc.ncifcrf.gov/) similar to previous report.[59] Moreover, thePPI network based on both the proteins found in 2-DE analysis and LC-MS was established as reported in our previous study.[55] Briefly, based on PPI database, Python programming language was used to fish out the direct partners interacting with our experimental proteins. Then, another round of partner proteins was also fished out. Through this way, the network was expanded step by step until all experimental proteins could be included into one network. Then, the network was clustered and simplified to a minimum network through the Steiner minimal tree algorithm. Finally, this network was export to pajek format. Further, to show the relationship between the proteins, proteins in the network were partitioned based on degree by pajek.

Regulation of GSK3β by celastrol and influence of GSK3β inhibitor on apoptosis induced by celastrol. The time-dependent change in levels of GSK3β and p-GSK3β (Ser 9) in cells treated with celastrol (1 μM) was examined using western blotting assay as described above. To check whether the change in GSK3β was caused by celastrol or just a consequence of cell death, the effects of topotecan, a classical apoptosis inducer, on GSK3β were also checked and compared with that of celastrol. Levels of GSK3β and p-GSK3β in cells treated with celastrol (1 μM) or topotecan (1 μM) for 48 h were checked using western blotting assay. The inhibitive effects of LiCL, a specific GSK3β inhibitor, on GSK3β were confirmed by checking the effects of LiCl (1, 2 or 5 mM for 1 h) on the level of p-GSK3β using western blotting assay. Apoptosis rate of celastrol-treated cells with or without pretreatment of LiCL (1 mM for 1 h) was examined using flow cytometry analysis as described above.

Statistical analysis. Values were expressed as mean ± S.D. The statistical significance of differences between control and treated groups was evaluated by a non-paired two-tailed Student's *t*-test (GraphPad Prism4). All comparisons are made relative to untreated controls and $P < 0.05$ was considered statistically significant. For each variable, three independent experiments were carried out unless otherwise indicated.

Conflict of Interest

The authors declare no conflict of interest.

Acknowledgements. We thank Dr. Qi Hou (Institute of Materia Medica, Chinese Academy of Medical Sciences and Peking Union Medical College) for the GFP-Bax plasmid. This work was supported in part by grants from Major Projects of Knowledge Innovation Program of the Chinese Academy of Sciences (Number: KSCX2-YW-R-166) and the Twelfth Five-Year National Science and Technology Support Program (Number: 2012BAI29B06), the National Natural Science Foundation of China (No.30960450) and Yunnan Provincial Science and Technology Department (No.2011FA022).

1. Liu Z, Ma L, Zhou GB. The main anticancer bullets of the Chinese medicinal herb, thunder god vine. *Molecules* 2011; **16**: 5283–5297.
2. Salminen A, Lehtonen M, Paimela T, Kaarniranta K. Celastrol: molecular targets of Thunder God Vine. *Biochem Biophys Res Commun* 2010; **394**: 439–442.
3. Ding QH, Cheng Y, Chen WP, Zhong HM, Wang XH. Celastrol, an inhibitor of heat shock protein 90beta potently suppresses the expression of matrix metalloproteinases, inducible nitric oxide synthase and cyclooxygenase-2 in primary human osteoarthritic chondrocytes. *Eur J Pharmacol* 2013; **708**: 1–7.
4. Chow AM, Tang DW, Hanif A, Brown IR. Induction of heat shock proteins in cerebral cortical cultures by celastrol. *Cell Stress Chaperones* 2013; **18**: 155–160.
5. Sreeramulu S, Gande SL, Gobel M, Schwalbe H. Molecular mechanism of inhibition of the human protein complex Hsp90-Cdc37, a kinome chaperone-cochaperone, by triterpene celastrol. *Angew Chem Int Ed Engl* 2009; **48**: 5853–5855.
6. Wang WB, Feng LX, Yue QX, Wu WY, Guan SH, Jiang BH *et al.* Paraptosis accompanied by autophagy and apoptosis was induced by celastrol, a natural compound with influence on proteasome, ER stress and Hsp90. *J Cell Physiol* 2012; **227**: 2196–2206.
7. Rajendran P, Li F, Shanmugam MK, Kannaiyan R, Goh JN, Wong KF *et al.* Celastrol suppresses growth and induces apoptosis of human hepatocellular carcinoma through the modulation of STAT3/JAK2 signaling cascade *in vitro* and *in vivo*. *Cancer Prev Res (Phila)* 2012; **5**: 631–643.
8. Li Z, Wu X, Li J, Yao L, Sun L, Shi Y *et al.* Antitumor activity of celastrol nanoparticles in a xenograft retinoblastoma tumor model. *Int J Nanomed* 2012; **7**: 2389–2398.
9. Zhou LL, Lin ZX, Fung KP, Cheng CH, Che CT, Zhao M *et al.* Celastrol-induced apoptosis in human HaCaT keratinocytes involves the inhibition of NF-kappaB activity. *Eur J Pharmacol* 2011; **670**: 399–408.

10. Yang HS, Kim JY, Lee JH, Lee BW, Park KH, Shim KH *et al.* Celastrol isolated from Tripterygium regelii induces apoptosis through both caspase-dependent and -independent pathways in human breast cancer cells. *Food Chem Toxicol* 2011; **49**: 527–532.
11. Tozawa K, Sagawa M, Kizaki M. Quinone methide tripterine, celastrol, induces apoptosis in human myeloma cells via NF-kappaB pathway. *Int J Oncol* 2011; **39**: 1117–1122.
12. Mou H, Zheng Y, Zhao P, Bao H, Fang W, Xu N. Celastrol induces apoptosis in non-small-cell lung cancer A549 cells through activation of mitochondria- and Fas/FasL-mediated pathways. *Toxicol In Vitro* 2011; **25**: 1027–1032.
13. Kannaiyan R, Manu KA, Chen L, Li F, Rajendran P, Subramaniam A *et al.* Celastrol inhibits tumor cell proliferation and promotes apoptosis through the activation of c-Jun N-terminal kinase and suppression of PI3 K/Akt signaling pathways. *Apoptosis* 2011; **16**: 1028–1041.
14. Lu Z, Jin Y, Qiu L, Lai Y, Pan J. Celastrol, a novel HSP90 inhibitor, depletes Bcr-Abl and induces apoptosis in imatinib-resistant chronic myelogenous leukemia cells harboring T315I mutation. *Cancer Lett* 2010; **290**: 182–191.
15. Ge P, Ji X, Ding Y, Wang X, Fu S, Meng F *et al.* Celastrol causes apoptosis and cell cycle arrest in rat glioma cells. *Neurol Res* 2010; **32**: 94–100.
16. Yang H, Chen D, Cui QC, Yuan X, Dou QP. Celastrol, a triterpene extracted from the Chinese "Thunder of God Vine," is a potent proteasome inhibitor and suppresses human prostate cancer growth in nude mice. *Cancer Res* 2006; **66**: 4758–4765.
17. Chapelsky S, Batty S, Frost M, Mogridge J. Inhibition of anthrax lethal toxin-induced cytolysis of RAW264.7 cells by celastrol. *PLoS One* 2008; **3**: e1421.
18. Chen M, Rose AE, Doudican N, Osman I, Orlow SJ. Celastrol synergistically enhances temozolomide cytotoxicity in melanoma cells. *Mol Cancer Res* 2009; **7**: 1946–1953.
19. Zhang D, Richardson DR. Endoplasmic reticulum protein 29 (ERp29): an emerging role in cancer. *Int J Biochem Cell Biol* 2011; **43**: 33–36.
20. Bambang IF, Xu S, Zhou J, Salto-Tellez M, Sethi SK, Zhang D. Overexpression of endoplasmic reticulum protein 29 regulates mesenchymal-epithelial transition and suppresses xenograft tumor growth of invasive breast cancer cells. *Lab Invest* 2009; **89**: 1229–1242.
21. Ma Y, Brewer JW, Diehl JA, Hendershot LM. Two distinct stress signaling pathways converge upon the CHOP promoter during the mammalian unfolded protein response. *J Mol Biol* 2002; **318**: 1351–1365.
22. Urano F, Wang X, Bertolotti A, Zhang Y, Chung P, Harding HP *et al.* Coupling of stress in the ER to activation of JNK protein kinases by transmembrane protein kinase IRE1. *Science* 2000; **287**: 664–666.
23. Harner M, Neupert W, Deponte M. Lateral release of proteins from the TOM complex into the outer membrane of mitochondria. *EMBO J* 2011; **30**: 3232–3241.
24. Ott M, Norberg E, Walter KM, Schreiner P, Kemper C, Rapaport D *et al.* The mitochondrial TOM complex is required for tBid/Bax-induced cytochrome c release. *J Biol Chem* 2007; **282**: 27633–27639.
25. Ott M, Norberg E, Zhivotovsky B, Orrenius S. Mitochondrial targeting of tBid/Bax: a role for the TOM complex? *Cell Death Differ* 2009; **16**: 1075–1082.
26. Bellot G, Cartron PF, Er E, Oliver L, Juin P, Armstrong LC *et al.* TOM22, a core component of the mitochondria outer membrane protein translocation pore, is a mitochondrial receptor for the proapoptotic protein Bax. *Cell Death Differ* 2007; **14**: 785–794.
27. Renault TT, Grandier-Vazeille X, Arokium H, Velours G, Camougrand N, Priault M *et al.* The cytosolic domain of human Tom22 modulates human Bax mitochondrial translocation and conformation in yeast. *FEBS Lett* 2012; **586**: 116–121.
28. Ross K, Rudel T, Kozjak-Pavlovic V. TOM-independent complex formation of Bax and Bak in mammalian mitochondria during TNFalpha-induced apoptosis. *Cell Death Differ* 2009; **16**: 697–707.
29. Soo KY, Atkin JD, Farg M, Walker AK, Horne MK, Nagley P. Bim links ER stress and apoptosis in cells expressing mutant SOD1 associated with amyotrophic lateral sclerosis. *PLoS One* 2012; **7**: e35413.
30. Puthalakath H, O'Reilly LA, Gunn P, Lee L, Kelly PN, Huntington ND *et al.* ER stress triggers apoptosis by activating BH3-only protein Bim. *Cell* 2007; **129**: 1337–1349.
31. Ghosh AP, Klocke BJ, Ballestas ME, Roth KA. CHOP potentially co-operates with FOXO3a in neuronal cells to regulate PUMA and BIM expression in response to ER stress. *PLoS One* 2012; **7**: e39586.
32. Plyte SE, Hughes K, Nikolakaki E, Pulverer BJ, Woodgett JR. Glycogen synthase kinase-3: functions in oncogenesis and development. *Biochim Biophys Acta* 1992; **1114**: 147–162.
33. Meares GP, Zmijewska AA, Jope RS. HSP105 interacts with GRP78 and GSK3 and promotes ER stress-induced caspase-3 activation. *Cell Signal* 2008; **20**: 347–358.
34. McAlpine CS, Bowes AJ, Khan MI, Shi Y, Werstuck GH. Endoplasmic reticulum stress and glycogen synthase kinase-3beta activation in apolipoprotein E-deficient mouse models of accelerated atherosclerosis. *Arterioscler Thromb Vasc Biol* 2012; **32**: 82–91.
35. Meares GP, Mines MA, Beurel E, Eom TY, Song L, Zmijewska AA *et al.* Glycogen synthase kinase-3 regulates endoplasmic reticulum (ER) stress-induced CHOP expression in neuronal cells. *Exp Cell Res* 2011; **317**: 1621–1628.
36. Luo J. Glycogen synthase kinase 3beta (GSK3beta) in tumorigenesis and cancer chemotherapy. *Cancer Lett* 2009; **273**: 194–200.
37. Miyashita K, Nakada M, Shakoori A, Ishigaki Y, Shimasaki T, Motoo Y *et al.* An emerging strategy for cancer treatment targeting aberrant glycogen synthase kinase 3 beta. *Anticancer Agents Med Chem* 2009; **9**: 1114–1122.
38. Grimes CA, Jope RS. The multifaceted roles of glycogen synthase kinase 3beta in cellular signaling. *Prog Neurobiol* 2001; **65**: 391–426.
39. Chou CH, Chou AK, Lin CC, Chen WJ, Wei CC, Yang MC *et al.* GSK3beta regulates Bcl2L12 and Bcl2L12A anti-apoptosis signaling in glioblastoma and is inhibited by LiCl. *Cell Cycle* 2012; **11**: 532–542.
40. De Sarno P, Bijur GN, Zmijewska AA, Li X, Jope RS. *In vivo* regulation of GSK3 phosphorylation by cholinergic and NMDA receptors. *Neurobiol Aging* 2006; **27**: 413–422.
41. Stambolic V, Ruel L, Woodgett JR. Lithium inhibits glycogen synthase kinase-3 activity and mimics wingless signalling in intact cells. *Curr Biol* 1996; **6**: 1664–1668.
42. Choi CH, Lee BH, Ahn SG, Oh SH. Proteasome inhibition-induced p38 MAPK/ERK signaling regulates autophagy and apoptosis through the dual phosphorylation of glycogen synthase kinase 3beta. *Biochem Biophys Res Commun* 2012; **418**: 759–764.
43. Song L, De Sarno P, Jope RS. Central role of glycogen synthase kinase-3beta in endoplasmic reticulum stress-induced caspase-3 activation. *J Biol Chem* 2002; **277**: 44701–44708.
44. Huang WC, Lin YS, Chen CL, Wang CY, Chiu WH, Lin CF. Glycogen synthase kinase-3beta mediates endoplasmic reticulum stress-induced lysosomal apoptosis in leukemia. *J Pharmacol Exp Ther* 2009; **329**: 524–531.
45. Sato S, Fujita N, Tsuruo T. Modulation of Akt kinase activity by binding to Hsp90. *Proc Natl Acad Sci USA* 2000; **97**: 10832–10837.
46. Zhang T, Hamza A, Cao X, Wang B, Yu S, Zhan CG *et al.* A novel Hsp90 inhibitor to disrupt Hsp90/Cdc37 complex against pancreatic cancer cells. *Mol Cancer Ther* 2008; **7**: 162–170.
47. Miura T, Tanno M. The mPTP and its regulatory proteins: final common targets of signalling pathways for protection against necrosis. *Cardiovasc Res* 2012; **94**: 181–189.
48. Bijur GN, Jope RS. Rapid accumulation of Akt in mitochondria following phosphatidylinositol 3-kinase activation. *J Neurochem* 2003; **87**: 1427–1435.
49. Linseman DA, Butts BD, Precht TA, Phelps RA, Le SS, Laessig TA *et al.* Glycogen synthase kinase-3beta phosphorylates Bax and promotes its mitochondrial localization during neuronal apoptosis. *J Neurosci* 2004; **24**: 9993–10002.
50. King TD, Bijur GN, Jope RS. Caspase-3 activation induced by inhibition of mitochondrial complex I is facilitated by glycogen synthase kinase-3beta and attenuated by lithium. *Brain Res* 2001; **919**: 106–114.
51. Yue QX, Xie FB, Guan SH, Ma C, Yang M, Jiang BH *et al.* Interaction of Ganoderma triterpenes with doxorubicin and proteomic characterization of the possible molecular targets of Ganoderma triterpenes. *Cancer Sci* 2008; **99**: 1461–1470.
52. Yi YJ, Manandhar G, Sutovsky M, Li R, Jonakova V, Oko R *et al.* Ubiquitin C-terminal hydrolase-activity is involved in sperm acrosomal function and anti-polyspermy defense during porcine fertilization. *Biol Reprod* 2007; **77**: 780–793.
53. Luo H, Zhang J, Cheung C, Suarez A, McManus BM, Yang D. Proteasome inhibition reduces coxsackievirus B3 replication in murine cardiomyocytes. *Am J Pathol* 2003; **163**: 381–385.
54. Abe K, Kobayashi N, Sode K, Ikebukuro K. Peptide ligand screening of alpha-synuclein aggregation modulators by in silico panning. *BMC Bioinformatics* 2007; **8**: 451.
55. Yue QX, Cao ZW, Guan SH, Liu XH, Tao L, Wu WY *et al.* Proteomics characterization of the cytotoxicity mechanism of ganoderic acid D and computer-automated estimation of the possible drug target network. *Mol Cell Proteomics* 2008; **7**: 949–961.
56. Nechushtan A, Smith CL, Hsu YT, Youle RJ. Conformation of the Bax C-terminus regulates subcellular location and cell death. *EMBO J* 1999; **18**: 2330–2341.
57. Hou Q, Hsu YT. Bax translocates from cytosol to mitochondria in cardiac cells during apoptosis: development of a GFP-Bax-stable H9c2 cell line for apoptosis analysis. *Am J Physiol Heart Circ Physiol* 2005; **289**: H477–H487.
58. Wang X, Olberding KE, White C, Li C. Bcl-2 proteins regulate ER membrane permeability to luminal proteins during ER stress-induced apoptosis. *Cell Death Differ* 2011; **18**: 38–47.
59. Dennis G Jr., Sherman BT, Hosack DA, Yang J, Gao W, Lane HC *et al.* DAVID: Database for Annotation, Visualization, and Integrated Discovery. *Genome Biol* 2003; **4**: P3.

Supplementary Information accompanies this paper on Cell Death and Disease website (http://www.nature.com/cddis)